A Robust Method for Controlling Grid-Connected Inverters in Weak Grids

Akhavan, Ali; Vasquez, Juan C.; Guerrero, Josep M.

Published in:
IEEE Transactions on Circuits and Systems II: Express Briefs

DOI (link to publication from Publisher):
10.1109/TCSII.2020.3033427

Publication date:
2021

Document Version
Accepted author manuscript, peer reviewed version

A Robust Method for Controlling Grid-Connected Inverters in Weak Grids

Ali Akhavan, *Member, IEEE,* Juan C. Vasquez, *Senior Member, IEEE,* and Josep M. Guerrero, *Fellow, IEEE*

***Abstract*- Stable operation of grid-connected converters with the *LCL* filter is essential. Variations of the grid impedance and consequently, variations of the resonance frequency, can push the system toward instability. Also, delay that comes from sampling and PWM, could worsen the stability condition. Thus, the control system should be designed by considering these non-ideal factors. To fill in this gap, this paper presents an effective but simple method based on biquad filter, which enhances the system robustness and guarantees the system stability in a varying grid impedance condition. Besides, the suggested technique is free from employing any active damping mechanism, which in turn, increases the reliability and reduces the cost. Finally, experimental results are provided to show the accuracy of the analysis and verify the proposed method.**

***Index Terms*— Active damping, *LCL*-filtered inverters, resonance, stability, weak grids.**

I. Introduction

Developing renewable energy systems have received special interest to increase the reliability and efficiency of the system. Inverters as interfacing equipment play an important role in transporting energy from renewable-based resources to the grid [1]. However, using a filter at the output of the inverter is necessary for mitigation the switching harmonics, where an *LCL* filter is a wise choice because of its better harmonic attenuation and lower size in comparison with other types of filters. However, this panacea does not come without any challenges. Basically, the resonance of *LCL* filters may make the system prone to instability. Therefore, damping methods should be employed to mitigate the resonance of *LCL* filters [2], [3]. To this end, passive and active damping methods can be employed. The passive ones provide an effective and reliable resonance mitigation at the cost of extra power losses. On the contrary, active damping methods present a better efficiency using manipulating the control system. However, the delay in digital systems that comes from sampling and PWM, affects the optimal performance of such a method.

Although single-loop control systems can work stably even without any passive or active damping methods under specific grid conditions, however, grid impedance variation that is a very common scenario in weak grids may put the inverter at the risk of instability [4]. Therefore, using damping methods is obligatory to make sure about the stability of the system against the grid impedance variations. To this end, amending the negative aspect of delay should be addressed effectively.

Many works have been done to stabilize an *LCL*-filtered inverter using active damping methods by taking delay's negative effect into consideration. Xin *et al.* [5] proposed a reciprocal of a notch filter to expand the stable region of active damping. Yet, designing the filter parameters is not straightforward. In [6], a high-pass filter is used along with the capacitor's current active damping feedback, which may amplify the high-frequency noises. In [7], a method based on shifting the sampling instance is proposed, which burdens the computational task. Li *et al.* [8] presented a repetitive-based method that amends the delay effect. However, the gain of the loop gain is infinite at the Nyquist frequency, which may make problems. Although effective, the mentioned methods and similar works complicate the control system with additional task effort. Besides, they normally need a double-loop control method, which may burden the computational effort and probably need additional sensors, which in turn, increases the cost. Therefore, using a simple but robust method for control of grid-connected inverters is demanded, immediately. Thus, the main contribution of this paper is devoted to provide a simple, yet highly robust control system for grid-connected inverters. To this end, a biquad filter is employed in a single-loop control system that can stabilize the inverter without any extra sensors.

II. System Overview

Fig. 1 shows the schematic of a three-phase *LCL*-filtered grid-connected inverter. Z_{L1}, Z_{L2}, $Z_{C,}$ and Z_{Lg} are the corresponding impedances of the *LCL* filter and grid, respectively as follows:

$$Z_{L1} = L_1 s,\ Z_{L2} = L_2 s,\ Z_C = \frac{1}{Cs},\ Z_{Lg} = L_g s\,. \tag{1}$$

In this schematic, the inverter-side current i_1 is controlled using a single-loop control system. It should be noted that the DC-link voltage is supposed to be constant for the sake of simplicity. Also, the bandwidth of phase-locked-loop (PLL) is tuned intentionally far lower than the control system, therefore, it could be neglected without significantly affecting the accuracy of the stability evaluation [9].

The proposed control block diagram of the system is depicted in Fig. 2, where $G_i(z)$ is a proportional-resonant (PR) current regulator, z^{-1} models the PWM and the computational delay [10]. Also, $G_h(s)$ models the zero-order-hold (ZOH), which causes the half-sample PWM delay, expressed as:

This work was funded by a Villum Investigator grant (no. 25920) from the Villum Fonden.

This article has been accepted for publication in a future issue of this journal, but has not been fully edited. Content may change prior to final publication. Citation information: DOI 10.1109/TCSII.2020.3033427, IEEE Transactions on Circuits and Systems II: Express Briefs

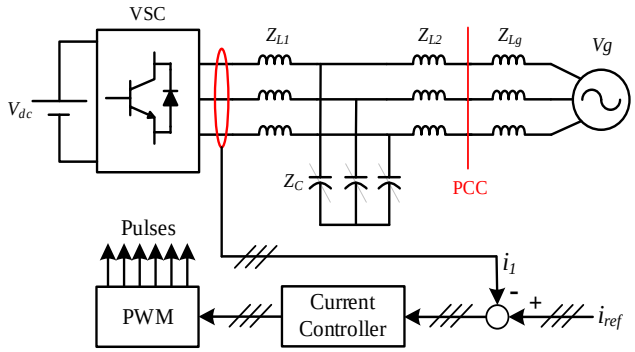

Fig. 1. The schematic of an *LCL*-filtered current-controlled inverter.

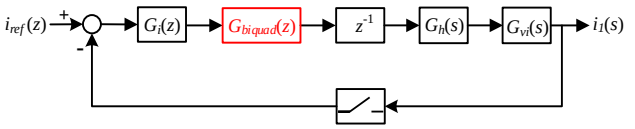

Fig. 2. The proposed single-loop control block diagram.

$$G_h(s) = \frac{1 - e^{-sT_s}}{s} \tag{2}$$

where T_s is the sampling period. Also, $G_{biquad}(z)$ is a digital filter that is used to stabilize the inverter under different grid impedance and will be introduced in the next section. $G_{vi}(s)$ is the transfer function between inverter output voltage $v_{inv}(s)$ and inverter-side current i_1, and it is expressed as:

$$G_{vi}(s) = \frac{i_1(s)}{v_{inv}(s)} = \frac{s^2(L_2 + L_g)C + 1}{s^3 L_1(L_2 + L_g)C + s(L_1 + L_2 + L_g)} \tag{3}$$

The resonant part of the PR regulator has no significant contribution on the frequencies far from the fundamental frequency. Therefore, the PR regulator could be regarded as a proportional gain at high frequencies for stability evaluation [11]. Hence, supposing $G_i(z) \approx k_p$, the system loop gain transfer function in the *z*-domain could be derived by applying ZOH transformation to $G_{vi}(s)$ as (4) as shown at the bottom of this page. In (4), $\omega_r = \sqrt{(L_1 + L_2 + L_g)/(L_1(L_2 + L_g)C)}$ is the *LCL* resonance angular frequency. Supposing $G_{biquad}(z) = 1$ and $L_g = 0$, the Bode diagram of $T(z)$ is illustrated in Fig. 3 with parameters presented in Table I. The system loop gain $T(z)$ has an anti-resonance peak at f_a and a resonance peak at f_r, which can be derived from (3) as follows:

$$f_a = \frac{1}{2\pi\sqrt{(L_2 + L_g)C}} \tag{5}$$

$$f_r = \frac{1}{2\pi}\sqrt{\frac{L_1 + L_2 + L_g}{L_1(L_2 + L_g)C}} \tag{6}$$

From Fig. 3, it could be easily found that the system is unstable since the phase plot crosses over −180° at f_r with an infinite resonance peak [2].

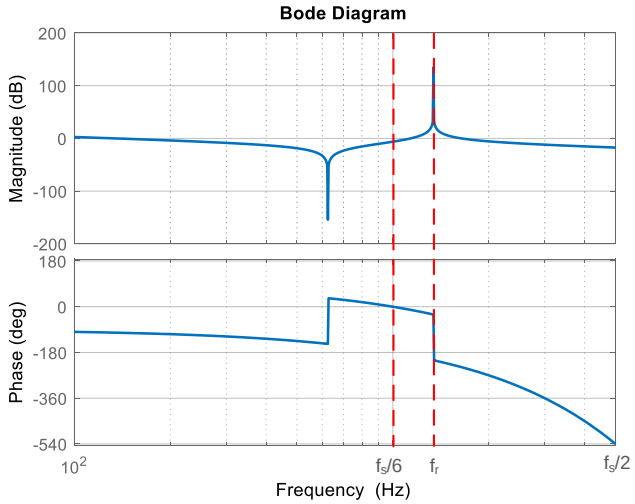

Fig. 3. The Bode diagram of the system loop gain.

TABLE I
System Parameters

DC-link voltage, V_{dc}	650 V
Inverter-side inductor, L_1	1 mH
Filter capacitor, C	18 µF
Grid-side inductor, L_2	3.6 mH
Sampling frequency	6 kHz
Rated power of the inverter	2.2 kVA
Grid Voltage, V_g	400 V (Line to line)
Frequency	50 Hz
Grid inductance, L_g	0 mH < L_g < 20 mH

Regarding the low magnitude of the Bode diagram of $T(z)$ at $f_s/6$, the system could be stable if a constant 180° phase lag is introduced at $f_s/6$. This phase lag could be satisfied easily by a biquad filter, which is explained in the next section.

III. Stability Improvement Using the Biquad Filter

The biquad filter equation that is used in this paper is presented in (7), in *s*-domain.

$$G_{biquad}(s) = \frac{\omega_p^2}{\omega_z^2} \cdot \frac{s^2 + \omega_z^2}{s^2 + \omega_p^2} \tag{7}$$

where $\omega_z = 2\pi f_z$ and $\omega_p = 2\pi f_p$ are resonant zeros and poles, respectively [12]. The frequency response of the biquad filter is plotted in Fig. 4, where $f_p < f_z$ is selected to introduce a negative 180° phase lag. It could be seen that the magnitude of the biquad filter yields a notch at f_z and a resonance at f_p. Also, the phase of the biquad filter keeps −180° in $f_p < f < f_z$ and changes to zero outside of this range. Thus, to perform an ideal phase shift, f_z should be set higher than $f_s/6$ and f_p should be set lower than $f_s/6$ to introduce a −180° phase shift at frequencies in the vicinity of $f_s/6$.

$$T(z) = \frac{k_p G_{biquad}(z)}{\omega_r L_1(L_1 + L_2 + L_g)} \cdot \frac{\omega_r L_1 T_s(z^2 - 2z\cos\omega_r T_s + 1) + (z-1)^2(L_2 + L_g)\sin\omega_r T_s}{z(z-1)(z^2 - 2z\cos\omega_r T_s + 1)} \tag{4}$$

This article has been accepted for publication in a future issue of this journal, but has not been fully edited. Content may change prior to final publication. Citation information: DOI 10.1109/TCSII.2020.3033427, IEEE Transactions on Circuits and Systems II: Express Briefs

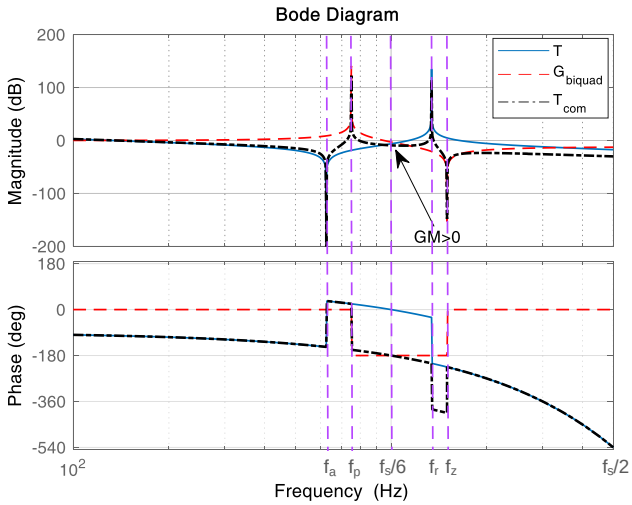

Fig. 4. The Bode diagrams of the uncompensated loop gain (T), biquad filter (G_{biquad}), and compensated loop gain (T_{com}).

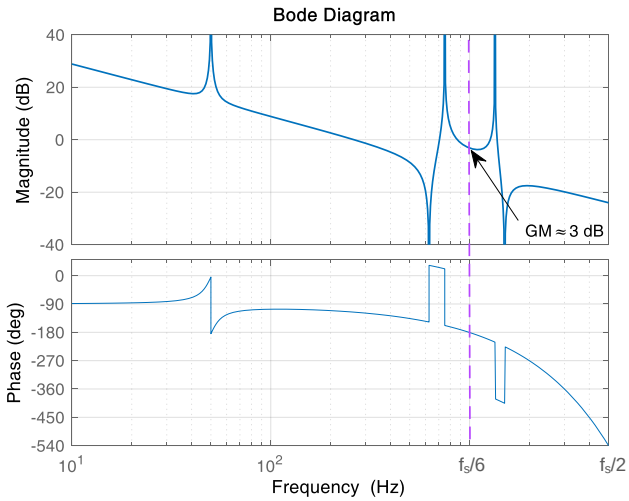

Fig. 5. The Bode diagram of the compensated loop gain (T_{com}) with parameters of Table II.

A. Desing of Biquad Filter Parameters

f_p should be set higher than f_a, otherwise, the phase lag of biquad filter causes instability because of negative gain margin (GM) when the phase plot crosses over −180º. Therefore, f_p should be tuned higher than the maximum possible value of f_a. Typically, the variations of capacitor and inductor are limited to ±10% and ±20%, respectively. Thus, referring to (5), the highest f_a is calculated when $L_g = 0$ as

$$f_a = \frac{1}{2\pi\sqrt{(0.8L_2+0)\cdot 0.9C}} = 1.18\cdot\frac{1}{2\pi\sqrt{L_2C}} \tag{8}$$

For the same reason, f_z should be set higher than the maximum possible value of f_r to guarantee stability. Therefore, referring to (6), the highest f_r is calculated when $L_g = 0$ as

$$f_r = \frac{1}{2\pi}\sqrt{\frac{0.8\cdot L_1+0.8\cdot L_2+0}{0.8\cdot L_1(0.8\cdot L_2+0)\cdot 0.9\cdot C}} = 1.18\cdot\frac{1}{2\pi}\sqrt{\frac{L_1+L_2}{L_1L_2C}} \tag{9}$$

Regarding (8), (9), and circuit parameters in Table I, f_p = 750 Hz and f_z = 1600 Hz are selected in this paper. The Bode diagram of the compensated loop gain (T_{com}) by considering the biquad filter is depicted in Fig. 4, as well. As it can be seen in this figure, T_{com} crosses −180º at $f_s/6$. By designing the current regulator to keep the magnitude of T_{com} smaller than 0 dB at $f_s/6$ (positive GM), the stability of the system guarantees.

B. Current Regulator Design

The proportional gain of the current regulator, k_p should be designed so that the system meets a desirable GM at $f_s/6$. Therefore, by considering the discretized biquad filter that is presented in (10) [12], the GM of the system at $f_s/6$ is expressed as (11) at the bottom of this page.

TABLE II
Control Parameters

Current regulator $G_i(z)$	
k_p	8
k_r	800
Biquad filter $G_{biquad}(z)$	
f_z	1500 Hz
f_p	750 Hz

$$G_{biquad}(z) = \frac{\omega_p^2}{\omega_z^2}\cdot\frac{z^2-2z\cos\omega_zT_s+1}{z^2-2z\cos\omega_pT_s+1} \tag{10}$$

Substituting f_z, f_p and the system parameters into (11) and letting GM($f_s/6$) > 3 dB, k_p < 8.6 is yielded. The gain of the resonant part (k_r) could be select to eliminate steady-state error and its role on the system stability could be neglected [13]. Thus, k_r = 800 is considered in this paper. Fig. 5 shows the Bode diagram of the compensated loop gain. It can be seen that all the stability constraints are well satisfied.

C. Stability Investigation Against Grid Impedance Variations

Regarding (11), the closed-loop poles map for compensated loop gain $T_{com}(z)$ is shown in Fig. 6, with L_g varying up to 23 mH, which corresponds to 10% per unit in the system. As shown in this figure, with the increase of grid inductance, poles of $T_{com}(z)$ move away from the unit circle to a more stable position. This result shows strong robustness against the grid impedance variations.

IV. Experimental Results

To confirm the validity of the proposed approach in different conditions, an experimental setup is built and control algorithm is implemented using *dSPACE* DS1006 platform.

$$\mathrm{GM}\big|_{f_s/6} = -20\log\left|T_z(e^{j\pi/3})\right| = 20\log\left|\frac{1}{k_p}\cdot\frac{\omega_z^2(1-2\cos\omega_pT_s)}{\omega_p^2(1-2\cos\omega_zT_s)}\cdot\frac{\omega_r(L_1+L_2+L_g)(1-2\cos\omega_rT_s)}{\sin\omega_rT_s+\omega_rT_s(1-2\cos\omega_rT_s)}\right| \tag{11}$$

This article has been accepted for publication in a future issue of this journal, but has not been fully edited. Content may change prior to final publication. Citation information: DOI 10.1109/TCSII.2020.3033427, IEEE Transactions on Circuits and Systems II: Express Briefs

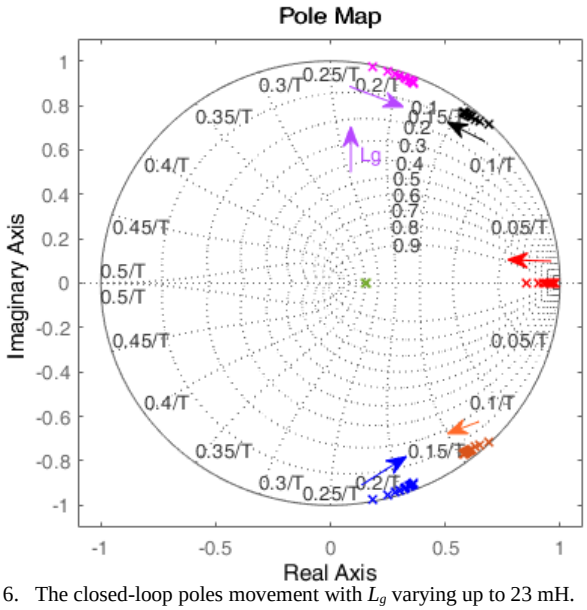

Fig. 6. The closed-loop poles movement with L_g varying up to 23 mH.

A. Validation of the Proposed Control System

Fig. 7 shows the current injected to the grid with L_g = 1.8 mH, where the resonance frequency is f_r = 1291 Hz. In this condition, $f_r > f_s/6$ and therefore, the single-loop control system is unstable. In this experiment, the proposed method is used at first, however, at t = 1s the biquad filter is disabled, and actually, the inverter works as a single-loop (uncompensated) control system. From Fig. 7, it is clear that the system works stably using the biquad filter. However, it goes toward instability when the biquad filter is disabled which is caused protective relays operation, consequently. The experimental results in this subsection show that the control system using the suggested approach is stable and can be used for control of inverters without any additional active damping mechanism. On the other hand, the single-loop control method is unstable when $f_r > f_s/6$.

B. Grid Impedance Variations

The capability of the control system under wide grid impedance variations is evaluated in this section. To this end, the grid inductance is swept from 0 to 20 mH with a step size of 5 mH. Series inductors between the inverter and grid-simulator *Chroma* act as a varying grid impedance for this test. The experimental results are shown in Fig. 8. From this figure, it is clear that the inverter can work stably irrespective of grid impedance wide variations. The experimental results confirm the analytical results concluded from Fig. 6 and show that system has a high robustness thanks to using the biquad filter.

C. Transient Response

To show the transient behavior of the system, a step-change in the reference current using the proposed method and the conventional active damping method that is used in [10] is applied, where L_g = 1.8 mH is considered and related results are shown in Figs. 9 and 10, respectively. It could be observed that, the proposed method has a better transient response and

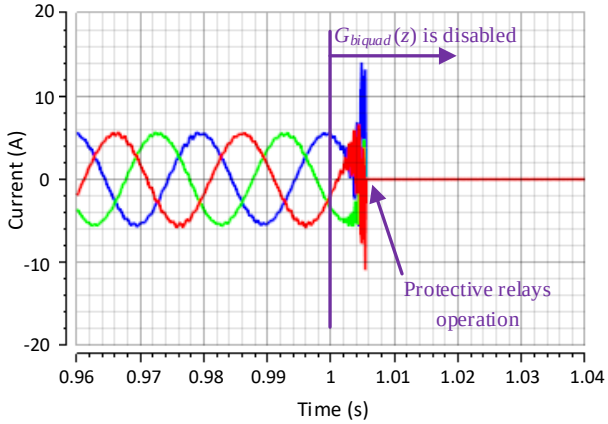

Fig. 7. The current injected to the grid using the proposed and single-loop control method.

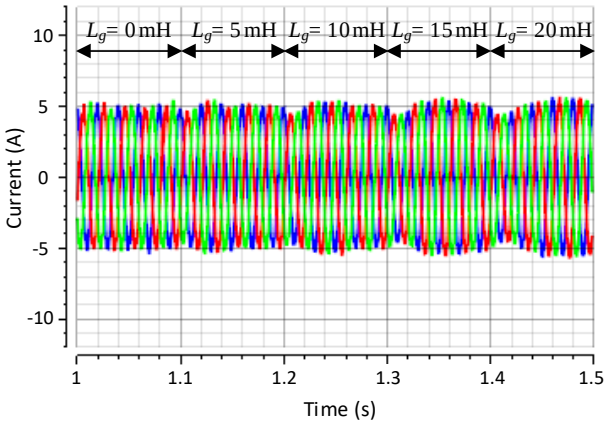

Fig. 8. The current injected to the grid using the proposed control method during the grid impedance wide variations.

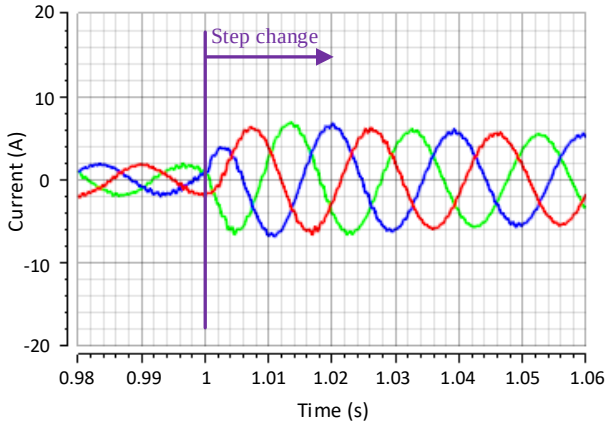

Fig. 9. The current injected to the grid using the proposed method during a step-change in the reference current.

reference tracking, since the control bandwidth of the single-loop control system could be deigned higher than conventional dual-loop active damping methods.

The experimental result for the case of 10% voltage sag (step change) is shown in Fig. 11, where the proposed method is employed. As shown in this figure, the grid-injected current backs to its reference after a short transient.

This article has been accepted for publication in a future issue of this journal, but has not been fully edited. Content may change prior to final publication. Citation information: DOI 10.1109/TCSII.2020.3033427, IEEE Transactions on Circuits and Systems II: Express Briefs

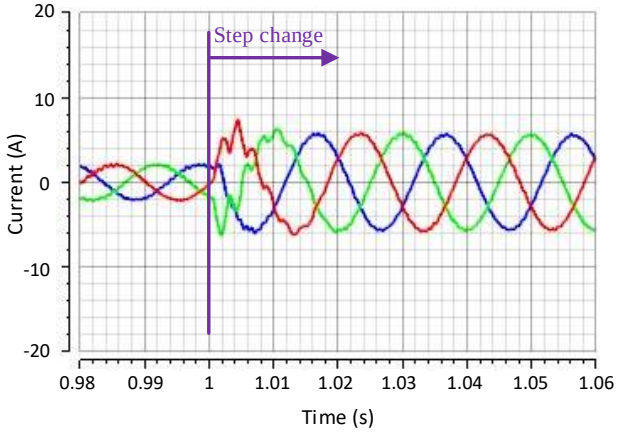

Fig. 10. The current injected to the grid using the method that is used in [10] during a step-change in the reference current.

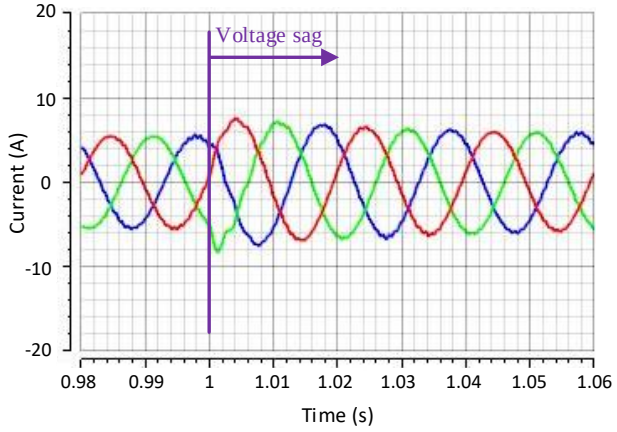

Fig. 11. The current injected to the grid during the voltage sag.

D. Multi-Paralleled inverters

In multi-paralleled systems, the interaction between parallel converters causes complex stability situation. In this condition, the equivalent grid impedance that each inverter sees, becomes different from the real grid impedance [14]. To evaluate the capability of the control system in multi-paralleled systems, the interconnection of two similar inverters with L_g = 1.8 mH is tested. Fig. 12 shows the total current injected to the grid. To this end, the first inverter is connected at first, and then, the second inverter connects to the grid. It could be observed in Fig. 12 that system keeps its stability even after connection of the second inverter.

V. Conclusion

This paper presents a simple yet, robust method to stabilized *LCL*-filtered grid-connected inverters. The proposed method is based on using a biquad filter along the main control loop. Thus, the system does not need double-loop control systems or any active damping mechanism, which in turn, increases the reliability and reduces the cost. Also, the design procedure of the system is very straightforward in this condition. The capability of the proposed method is validated using different case studies.

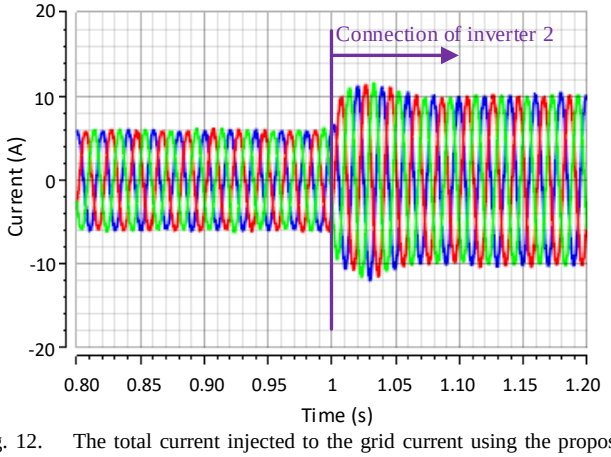

Fig. 12. The total current injected to the grid current using the proposed control system.

References

[1] Y. Deng, Y. Tao, G. Chen, G. Li, and X. He, "Enhanced power flow control for grid-connected droop-controlled inverters with improved stability," *IEEE Trans. Ind. Electron.*, vol. 64, no. 7, pp. 5919-5929, Jul. 2017.

[2] X. Ruan, X. Wang, D. Pan, D. Yang, W.i Li, and C. Bao, "Resonance damping methods of *LCL* filter," in *Control Techniques for LCL-Type Grid-Connected Inverters*, Beijing: Springer, 2018.

[3] Y. Han, M. Yang, H. Li, P. Yang, L. Xu, E. A. A. Coelho, and J. M. Guerrero "Modeling and stability analysis of *LCL*-type grid-connected inverters: A comprehensive overview, " in *IEEE Access*, vol. 7, pp. 114975-115001, 2019.

[4] X. Wang, F. Blaabjerg, and P. C. Loh, "Passivity-based stability analysis and damping injection for multiparalleled VSCs with *LCL* filters," *IEEE Trans. Power Electron*, vol. 32, no. 11, pp. 8922-8935, Nov. 2017.

[5] Z. Xin, X. Wang, P. C. Loh, and F. Blaabjerg, "Grid-current-feedback control for *LCL*-filtered grid converters with enhanced stability," *IEEE Trans. Power Electron.*, vol. 32, no. 4, pp. 3216-3228, Apr. 2017.

[6] X. Wang, F. Blaabjerg, and P. C. Loh, "Virtual *RC* damping of *LCL*-filtered voltage source converters with extended selective harmonic compensation," *IEEE Trans. Power Electron.*, vol. 30, no. 9, pp. 4726–4737, Sep. 2015.

[7] D. Pan, X. Ruan, C. Bao, W. Li, and X. Wang, "Capacitor-current-feedback active damping with reduced computation delay for improving robustness of *LCL*-type grid-connected inverter," *IEEE Trans. Power Electron.*, vol. 29, no. 7, pp. 3414–3427, Jul. 2014.

[8] X. Li, X. W. Y. Geng, X. Yuan, C. Xia, and X. Zhang, "Wide damping region for *LCL*-type grid-connected inverter with an improved capacitor current-feedback method," *IEEE Trans. Power Electron.*, vol. 30, no. 9, pp. 5247–5259, Sep. 2015.

[9] M. K. Bakhshizadeh, X. Wang, F. Blaabjerg, L. Kocewiak, C. L. Bak, and B. Hesselbak, "Coupling in phase domain impedance modelling of grid-connected converters," *IEEE Trans. Power Electron.*, vol. 31, no. 10, pp. 6792–6796, Oct. 2016.

[10] A. Akhavan, J. C. Vasquez, and J. M. Guerrero, "A simple method for passivity enhancement of current controlled grid-connected inverters," *IEEE Trans. Power Electron.*, vol. 35, no. 8, pp. 7735–7741, Aug. 2020.

[11] A. Kuperman, "Proportional-resonant current controllers design based on desired transient performance," *IEEE Trans. Power Electron.*, vol. 30, no. 10, pp. 5341-5345, Oct. 2015.

[12] D. Pan, X. Wang, F. Blaabjerg, and H. Gong, "Active damping of *LCL*-filter resonance using a digital resonant-notch (biquad) filter," in *2018 20th European Conference on Power Electronics and Applications* (*EPE'18 ECCE Europe*), Sept 2018, pp. 1–9.

[13] A. Akhavan, H. R. Mohammadi, J. C. Vasquez, and J. M. Guerrero, "Stability improvement of converter-side current controlled grid-connected inverters," in *Proc. 45th Annual Conference of the IEEE Industrial Electronics Society*, 2019, pp. 3943–3948.

[14] J. L. Agorreta, M. Borrega, J. López, and L. Marroyo, "Modeling and control of *N*-paralleled grid-connected inverters with *LCL* filter coupled due to grid impedance in PV plants," *IEEE Trans. Power Electron.*, vol. 26, no. 3, pp. 770-785, Mar. 2011.